Galactosylated IgG1 links FcγRIIB and Dectin-1 to block complement-mediated inflammation

Christian M. Karsten, Manoj K. Pandey, Julia Figge, Regina Kilchenstein, Philip R. Taylor, Marcela Rosas, Jacqueline U. McDonald, Selinda J. Orr, Markus Berger, Dominique Petzold, Veroniqué Blanchard, André Winkler, Constanze Hess, Delyth M. Reid, Irina V. Majoul, Richard T. Strait, Nathaniel L. Harris, Gabriele Köhl, Eva Wex, Ralf Ludwig[1], Detlef Zillikens[1], Falk Nimmerjahn, Fred D. Finkelman, Gordon D. Brown, Marc Ehlers & Jörg Köhl

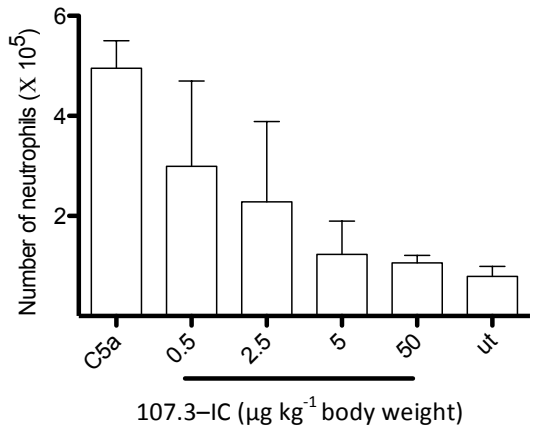

Supplementary Figure 1. IgG1–IC suppress C5a-mediated peritoneal inflammation in a dose-dependent manner. BALB/c WT mice were treated i.v. with the indicated concentrations of 107.3–IC 30 min prior to the i.p. injection of C5a (2 x 10^{-7}M). Our data suggest a broad dynamic range of inhibition starting at <0.5 μg kg^{-1} body weight and reaching a maximum of inhibition at 5 μg kg^{-1} body weight. Data are means ± s.e.m. (*n*=5-8/group).

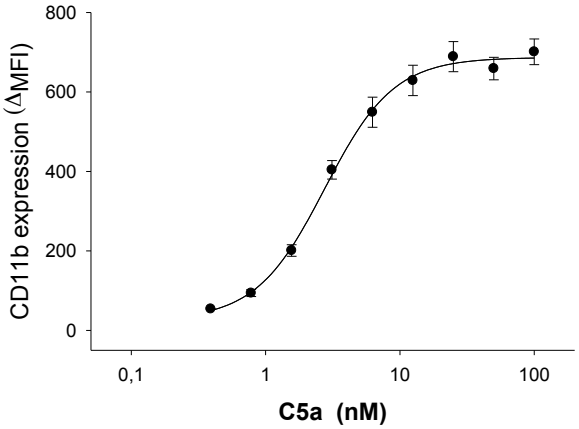

Supplementary Figure 2. C5a promotes upregulation of CD11b expression in BM neutrophils. BM cells from *Fcer1g*$^{-/-}$ mice were incubated with increasing concentrations of rhC5a. BM neutrophils were defined as in Fig. 1g by their FSC/SSC pattern and the expression of the Gr-1 marker. The increase in CD11b expression on BM neutrophils was calculated as the mean fluorescence intensity (MFI) in the presence of C5a – the MFI measured in the absence of C5a (=ΔMFI). Data are means ± s.e.m. (*n*=3).

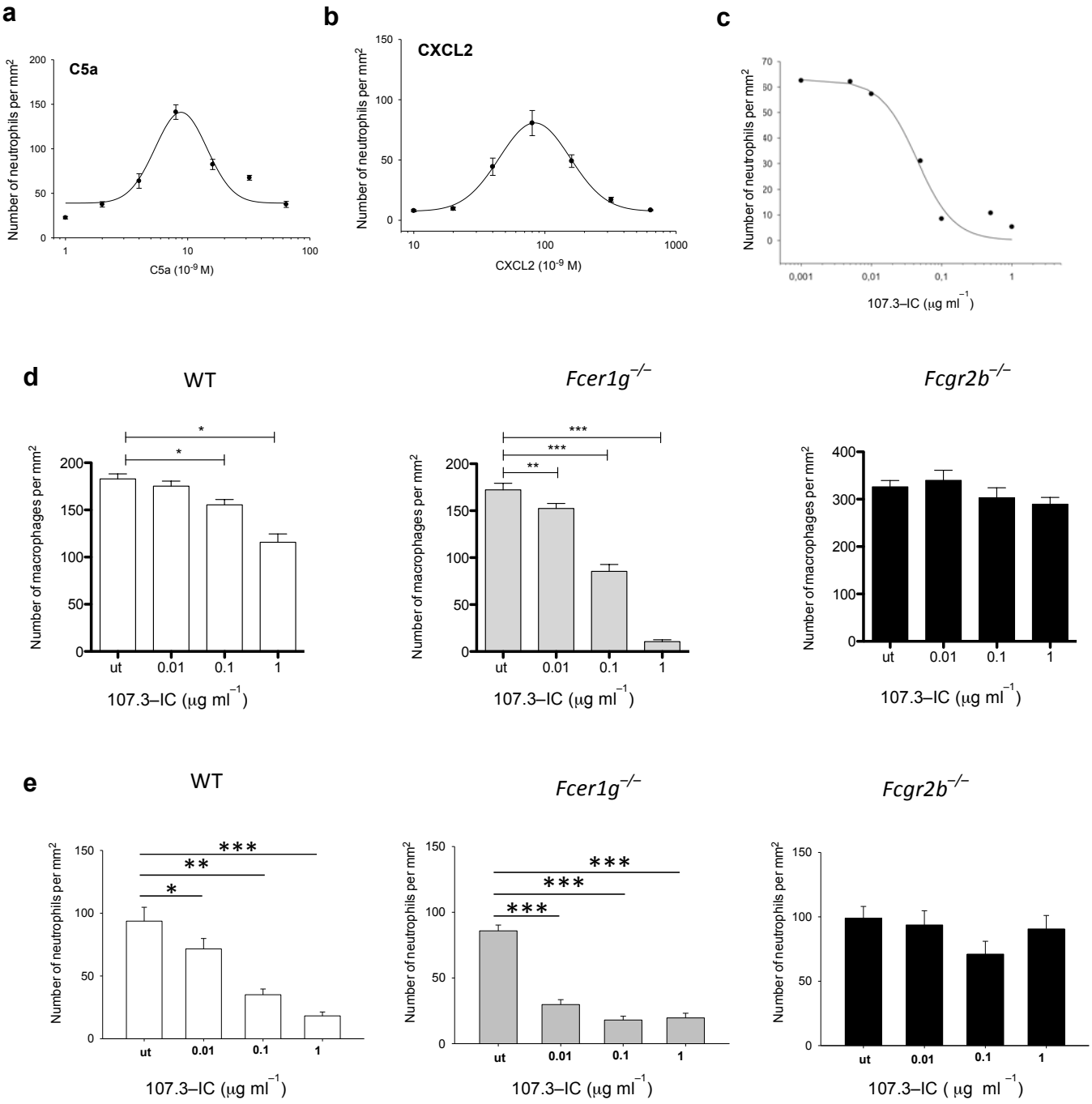

Supplementary Figure 3. Migration of BM neutrophils or peritoneal (PE) macrophages towards C5a and CXCL2 and the impact of 107.3–IC on cell migration. BM cells were incubated for 30 min with the indicated concentrations of (**a**) C5a or (**b**) CXCL2. (**c**) Typical dose response curve for the inhibitory effect of 107.3–IC on C5a (10^{-8}M)-mediated migration of BM-neutrophils from WT mice. We calculated a half-maximal inhibitory concentration (IC_{50}) of 0.048 μg ml^{-1} by three-parameter sigmoidal curve fitting. Peritoneal macrophages (**d**) or BM cells (**e**) were pre-incubated with the indicated concentration of 107.3–IC. Then, cells were allowed to migrate towards (**d**) C5a (10^{-8} M) or (**e**) CXCL2 (10^{-7}M) for 30min. 107.3–IC inhibit C5a or CXCL2-mediated migration of cells from WT and *Fcerg1*$^{-/-}$ but not from *Fcgr2b*$^{-/-}$ mice (*n*=5/group). Data are means ± s.e.m. * *P*<0.05, ** *P*<0.01, *** *P*<0.001.

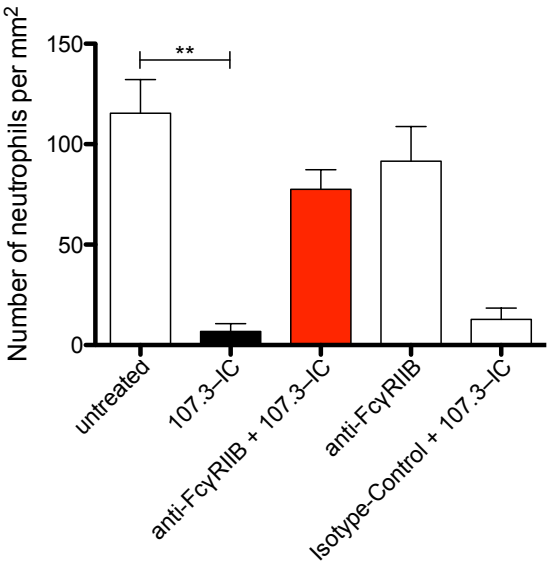

Supplementary Figure 4. Pharmacological targeting of FcγRIIB blocks the inhibitory effect of IgG1–IC on C5a-mediated neutrophil migration. BM cells from C57BL/6 *Fcer1g*$^{-/-}$ mice were preincubated with 0.5 μg ml^{-1} FcγRIIB-specific Ab (Ly17.2) or PBS for 30 min, followed by a 30 min incubation with 107.3–IC (0.1 μg ml^{-1}) or with PBS. Pretreatment of BM cells with the FcγRIIB-specific Ab abolished the inhibitory effect of the IgG1–IC (*n*=3/group). Data are means ± s.e.m. ** *P*<0.01.

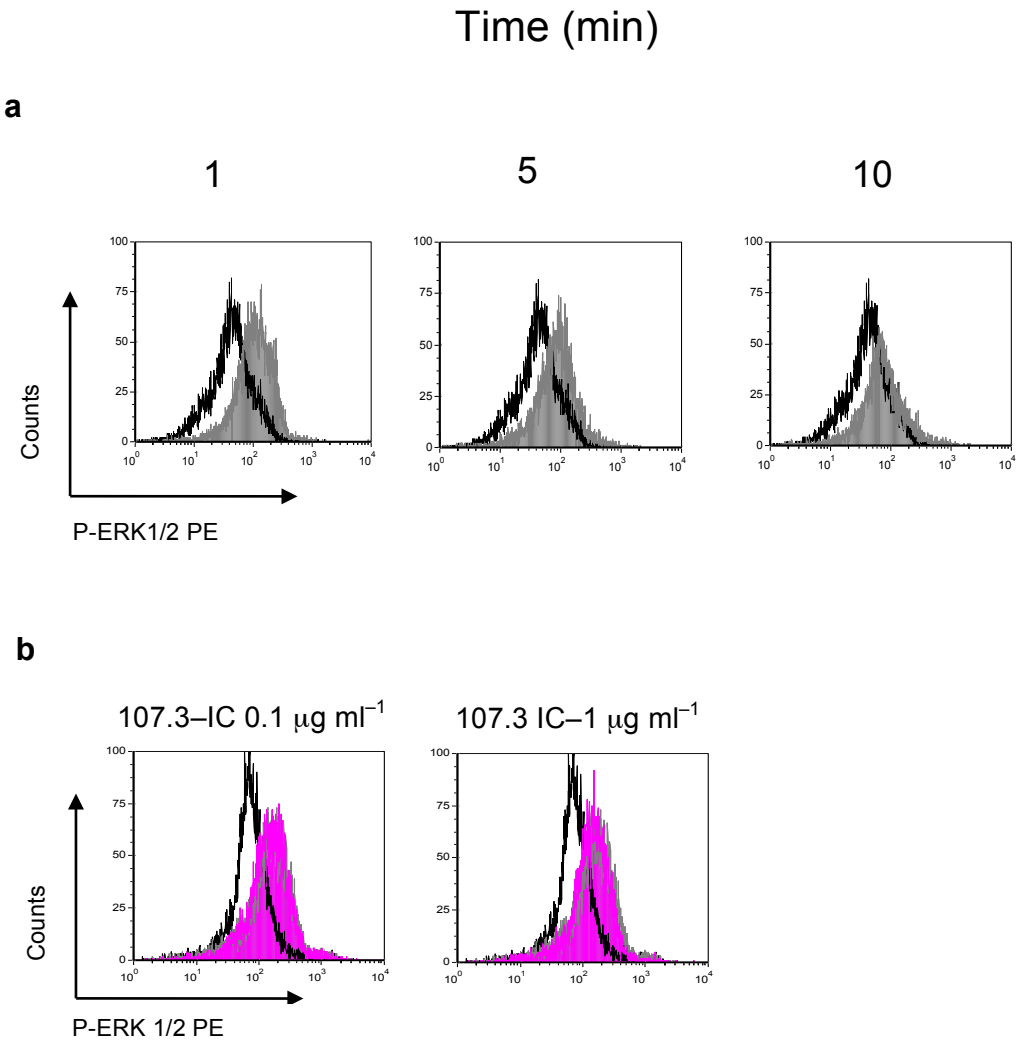

Supplementary Figure 5. Kinetics of C5a-mediated ERK1/2 phosphorylation in BM-derived Gr-1$^+$ neutrophils from WT mice and the impact of 107.3–IC treatment on ERK phosphorylation of neutrophils from *Fcgr2b*$^{-/-}$ mice. (**a**) BM cells from WT mice were incubated with rhC5a (50 nM) for the indicated times. To determine C5a-mediated ERK1/2 phosphorylation, cells were first gated on Gr-1$^+$ neutrophils and analyzed using a PE-labeled p-ERK1/2-specific Ab. The maximum ERK phosphorylation occurred already one min after C5a treatment and steadily declined during the next 9min. (**b**) BM cells from *Fcgr2b*-deficient mice were incubated for 30min with the indicated concentrations of 107.3–IC. Then, BM cells were stimulated for one min with C5a and ERK phosphorylation of Gr1^{hi} neutrophils was assessed. White histogram: ERK phosphorylation in the absence of C5a (background); grey histogram: ERK phosphorylation in response to C5a; magenta histogram: ERK phosphorylation in response to C5a and the indicated concentrations of 107.3–IC. Results in **a** and **b** are representative of three independent experiments.

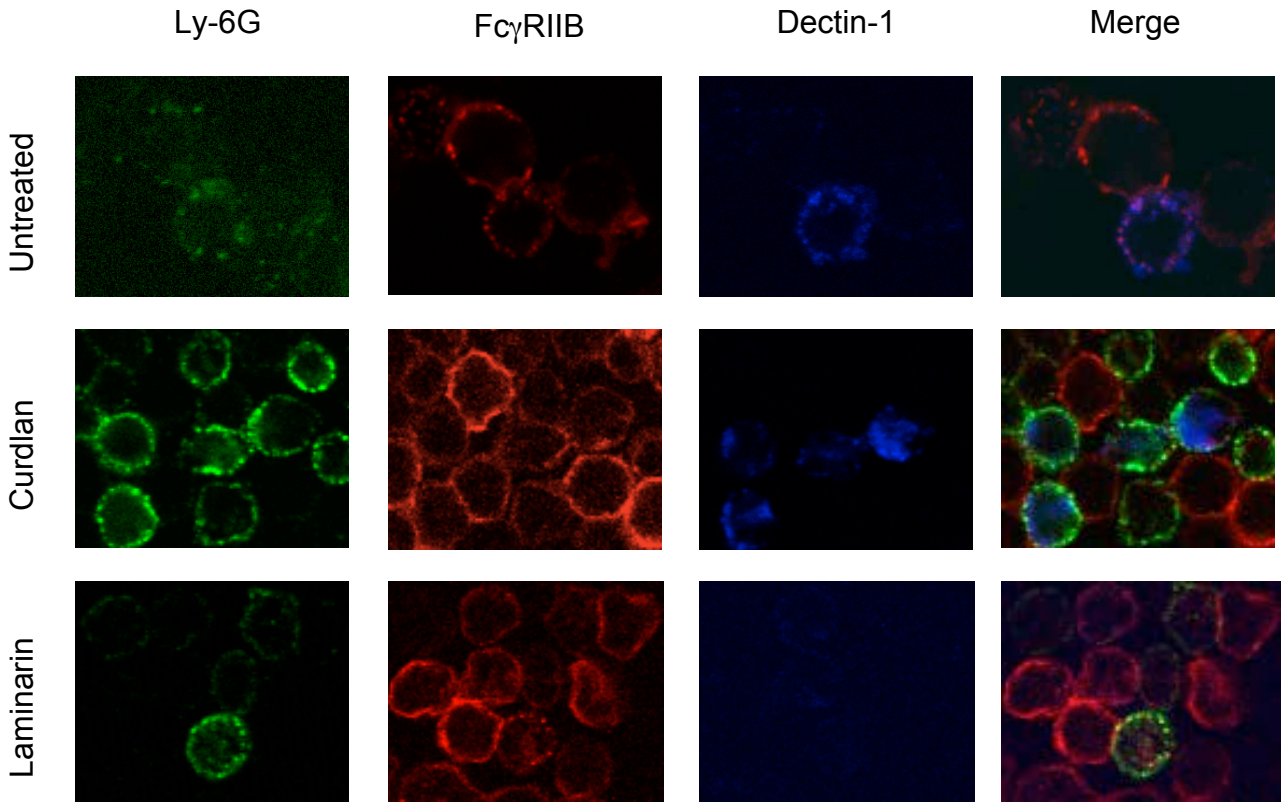

Supplementary Figure 6. Curdlan drives rapid internalization of Dectin-1 in BM neutrophils. BM-derived cells were stained for Ly-6G (green, FITC), FcγRIIB (red, PE) and Dectin-1 (blue, Alexa647). Then, such cells were incubated with 10 μg ml^{-1} curdlan or laminarin for 30 min at 37°C, washed and pictures were recorded using an Olympus FV 1000 laser scanning microscope. Curdlan treatment leads to internalization of Dectin-1 whereas laminarin displaces the anti-Dectin-1 Ab. Results are representative of at least three independent experiments.

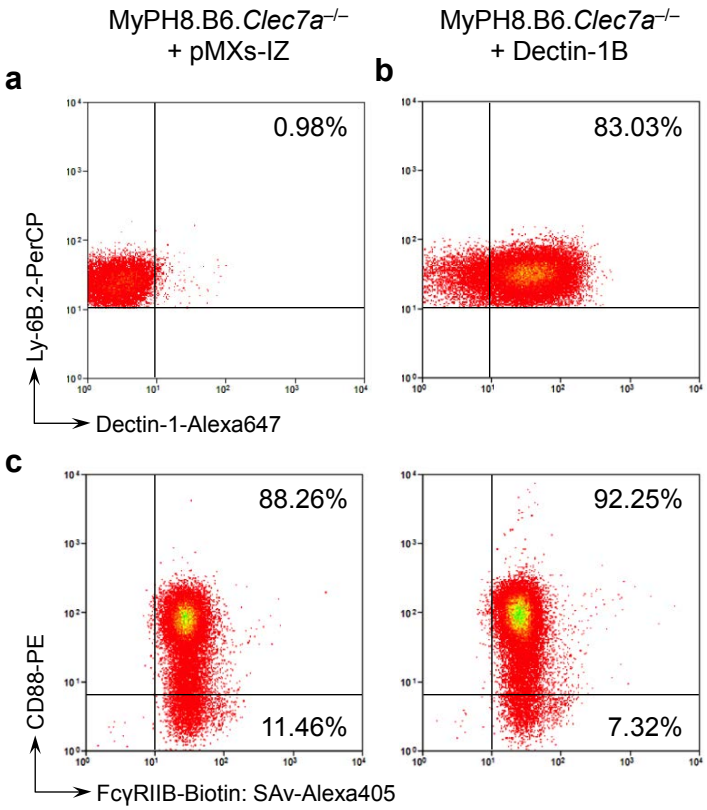

Supplementary Figure 7. Phenotypic characteristics of the *Clec7a*-deficient neutrophil cell line MyPH8-B6.*Clec7a*$^{-/-}$. (**a**) Neutrophils derived *in vitro* from MyPH8-B6.*Clec7a*$^{-/-}$ cells, retrovirally transduced with vector pMXs-IZ express no Dectin-1. (**b**) Following retroviral transduction with the Dectin-1B isoform, the *in vitro*-derived neutrophils from MyPH8-B6.*Clec7a*$^{-/-}$ cells express Dectin-1. (**c**) MyPH8-B6.*Clec7a*$^{-/-}$ cells express C5aR and FcγRIIB independent of whether they are transduced with vector pMXs-IZ (left panel) or with Dectin-1B (right panel). MyPH8-B6.*Clec7a*$^{-/-}$ cells were gated on Ly-6B.2^{+} *in vitro*-generated neutrophils. Samples were acquired on a CyAn ADP analyser (3 laser) (Beckman-Coulter) and analyzed using Summit software (Beckman-Coulter).

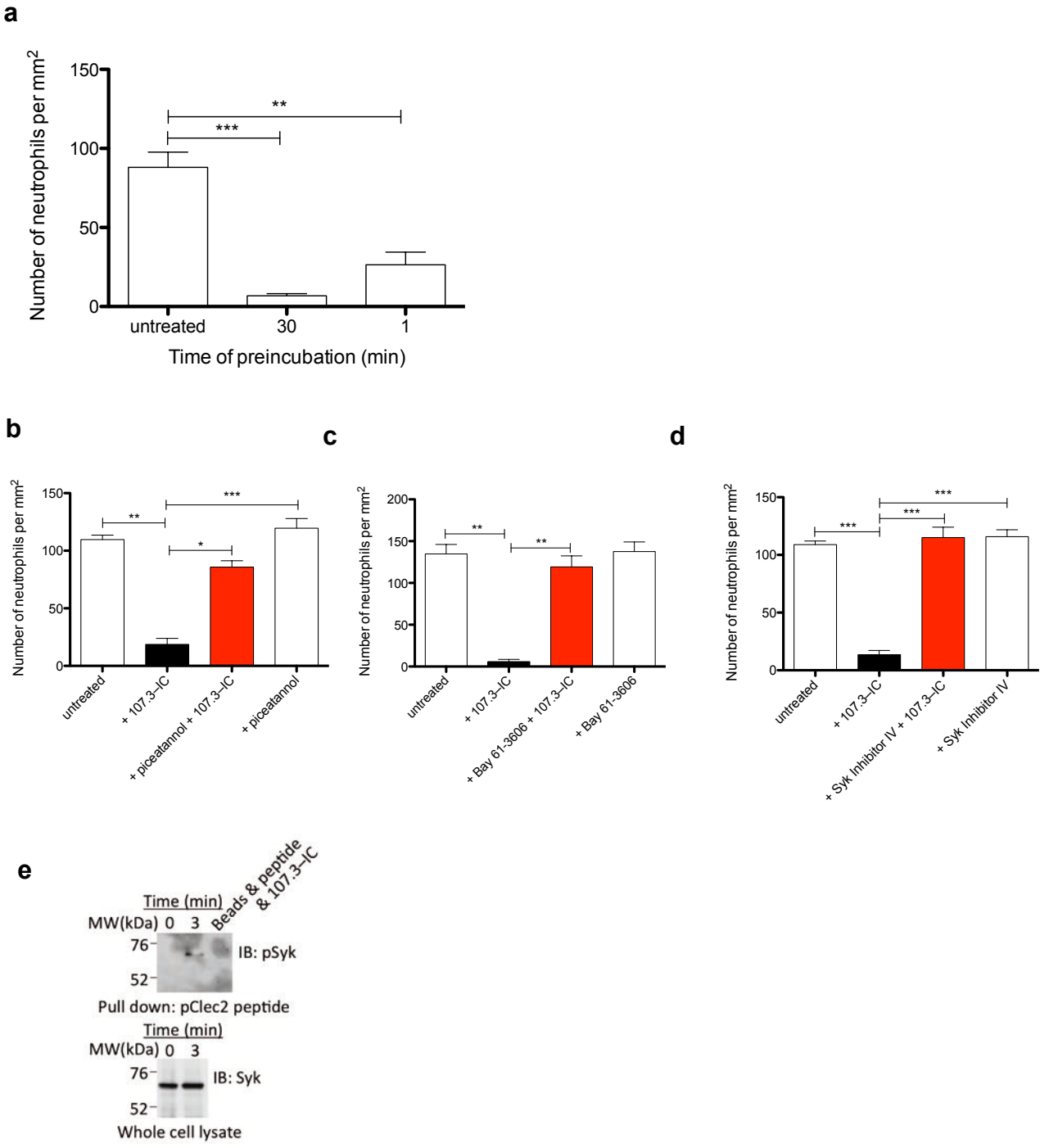

Supplementary Figure 8. Impact of preincubation time, tyrosine and Syk kinase activity on the inhibitory effect of IgG1–IC and pull-down of p-Syk with a Syk-binding phospho-petide. (**a**) BM cells from WT mice were preincubated with 107.3–IC (0.1 μg ml^{-1}) for the indicated times. 107.3–IC significantly inhibit C5a-mediated chemotaxis of BM cells after only one min of preincubation. Specific blockade of Syk tyrosine kinase using (**b**) piceatannol, (**c**) Bay 61-3606, or (**d**) Syk inhibitor IV (all at 10 μM) reversed the inhibitory effect of 107.3–IC (0.1 μg ml^{-1}). (*n*=3-5/group). Data are means ± s.e.m. * *P*<0.05, ** *P*<0.01, *** *P*<0.001. (**e**) Representative peptide pull-down (pClec2 peptide[21]) experiment showing 107.3 IC-driven phosphorylation of Syk in a *Clec7a*$^{-/-}$ neutrophil cell line transfected with Dectin-1B isoform. Data are representative of two independent experiments.

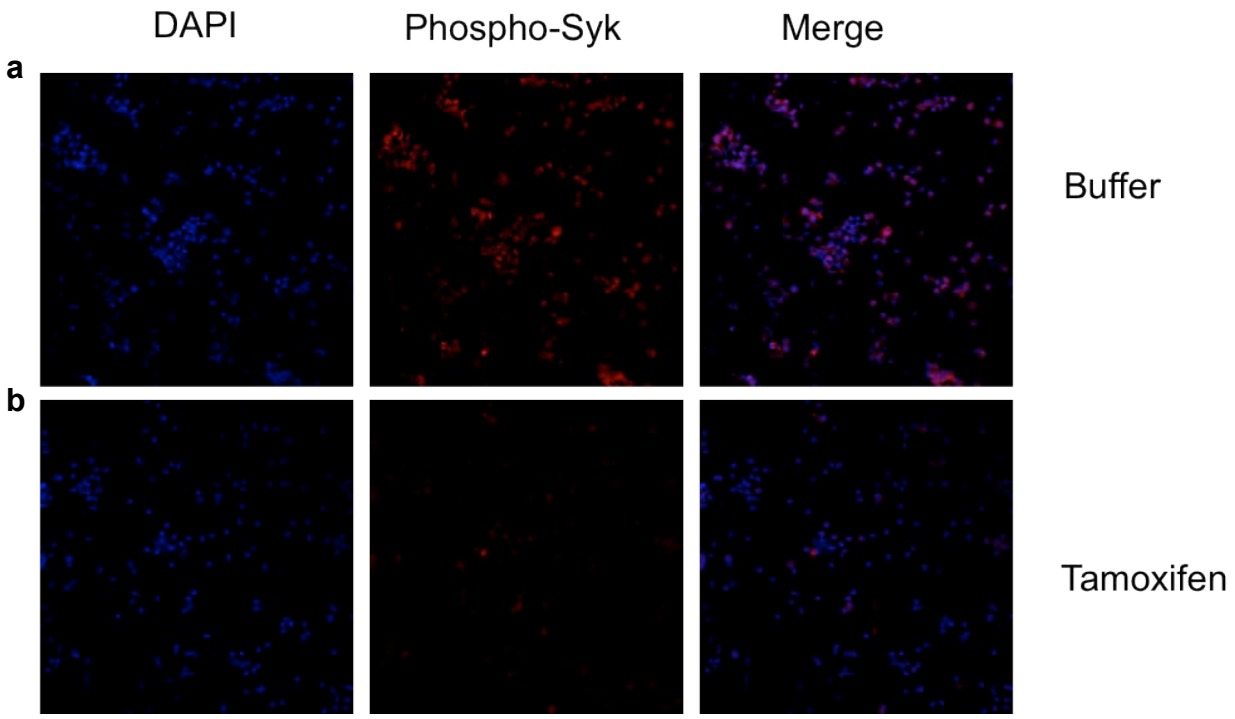

Supplementary Figure 9. Tamoxifen treatment of BM cells from conditional Syk knockout mice results in functional Syk depletion. We used inducible Syk knockout mice ($Syk^{flox/flox}$) that comprise a floxed Syk gene and a tamoxifen-inducible Cre recombinase under the control of the ubiquitously active Rosa26-promoter. (**a**) BM cells from such mice were cultured in RPMI for 48h. Then they were treated with 10 μg ml^{-1} of the Dectin-1 agonist curdlan. This treament resulted in strong phosphorylation of Syk after 3 min. (**b**) Addition of tamoxifen during the 48h culture abrogated the curdlan-induced phosphorylation of Syk. Results are representative of three independent experiments.

a

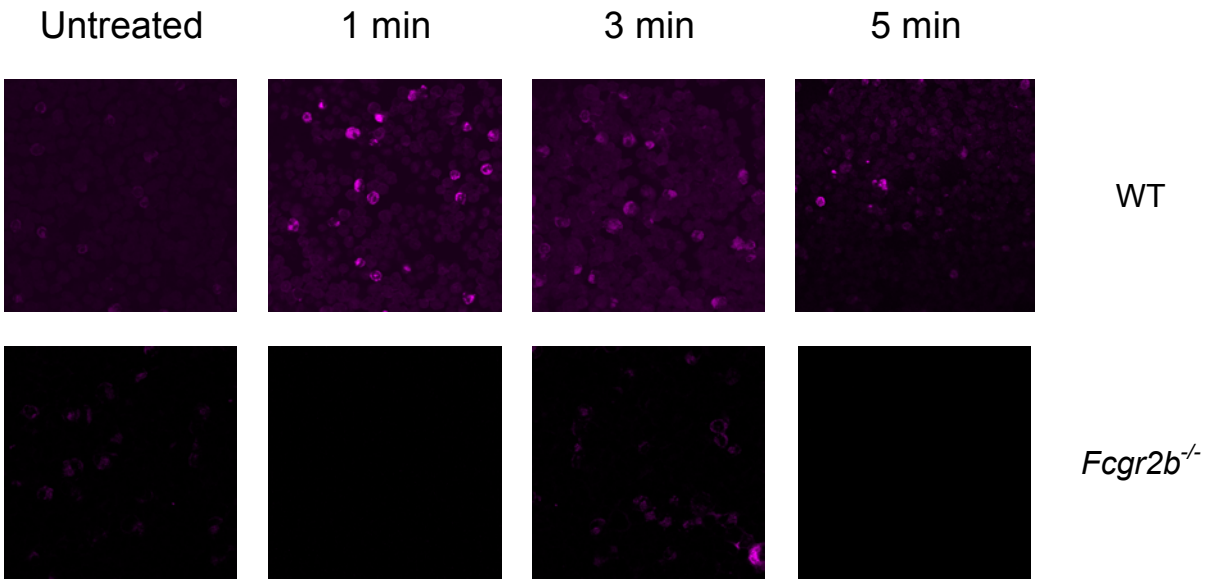

b

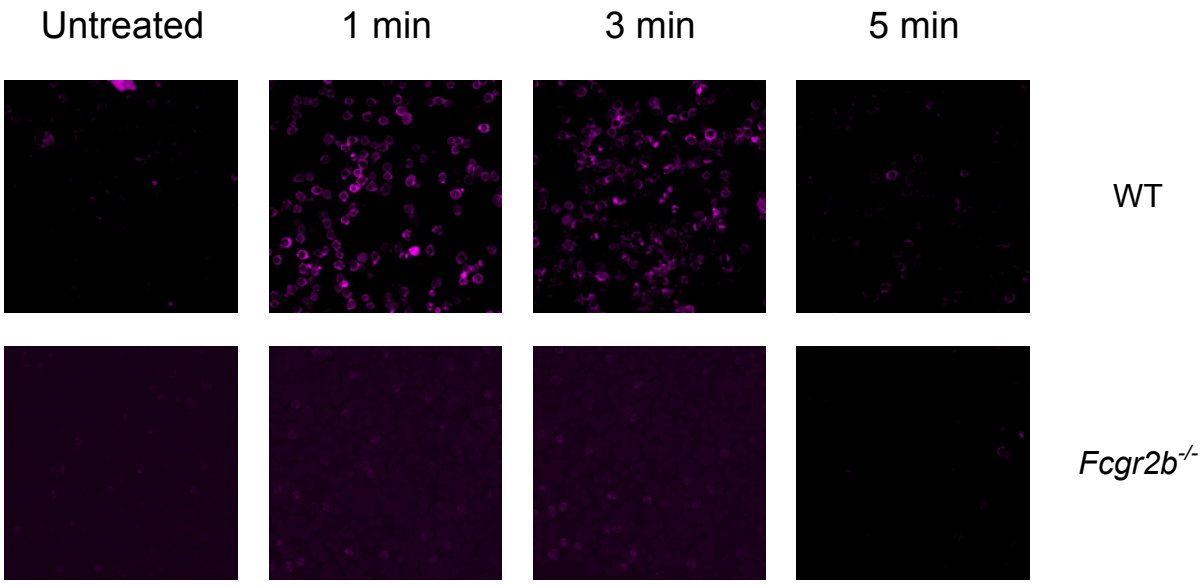

Supplementary Figure 10. 107.3–IC promote transient phosphorylation of Syk and SHIP. BM cells from BALB/c WT or *Fcgr2b*$^{-/-}$ mice were incubated with 107.3–IC for the indicated times. Untreated BM neutrophils show no (**a**) Syk or (**b**) SHIP phosphorylation. In, contrast, 107.3–IC treatment for one or three min induced (**a**) Syk or (**b**) SHIP phosphorylation which declined after 5min. Results in **a** and **b** are representative of at least three independent experiments.

Fc glycan 2D structure	Mass (m/z)
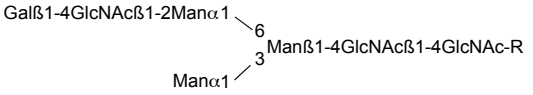	1620.8
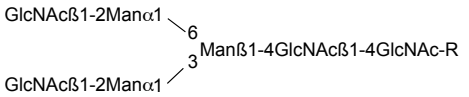	1661.8
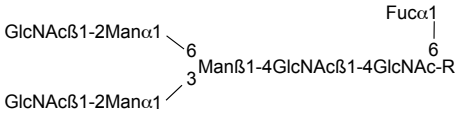	1835.9
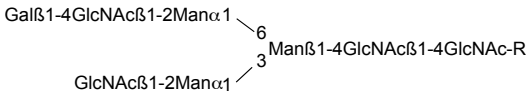	1865.9
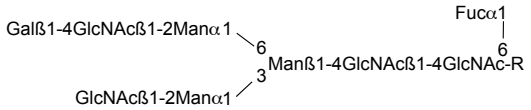	2040.0
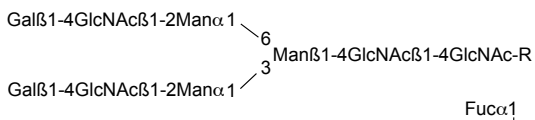	2070.0
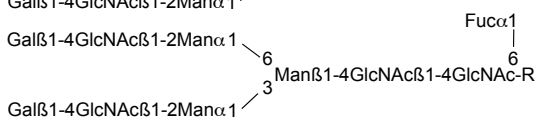	2244.1
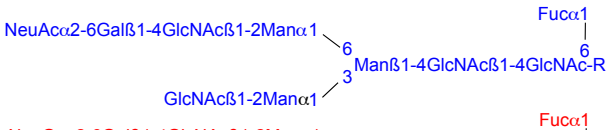	2401.1
	2431.2
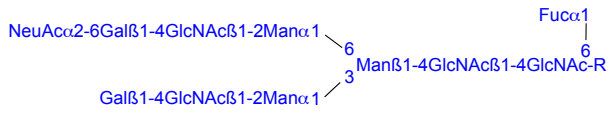	2605.2
	2636.2
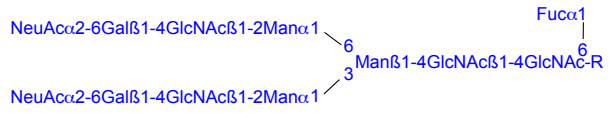	2967.3
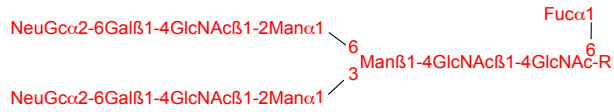	3026.5

Supplementary Figure 11. Relevant N-glycans found in this study. N-glycans are formed of a pentasaccharide core structure (GlcNAc2Man3). The heterogeneity of these N-glycans derives from additions of GlcNAc, Gal and all sialic acids (N-acetylneuraminic acid (NeuAc) mediated by human sialyltransferases or N-glycolylneuraminic acid by mouse sialytransferases (NeuGc). We show mono-galactosylation only on the alpha1,6 branch or mono-sialylation on the alpha2,6 branch as examples. In antibodies, core fucosylation occurs only with an alpha1,6 linkage. Species differences are indicated by colors (human=blue and mouse=red). The numbers show the molecular mass of the distinct N-glycan structures released upon PNGase F treatment as determined by MALDI-TOF. The molecular mass of 3026.5 for the G2S2 structure is the calculated mass. Fuc: (fucose).

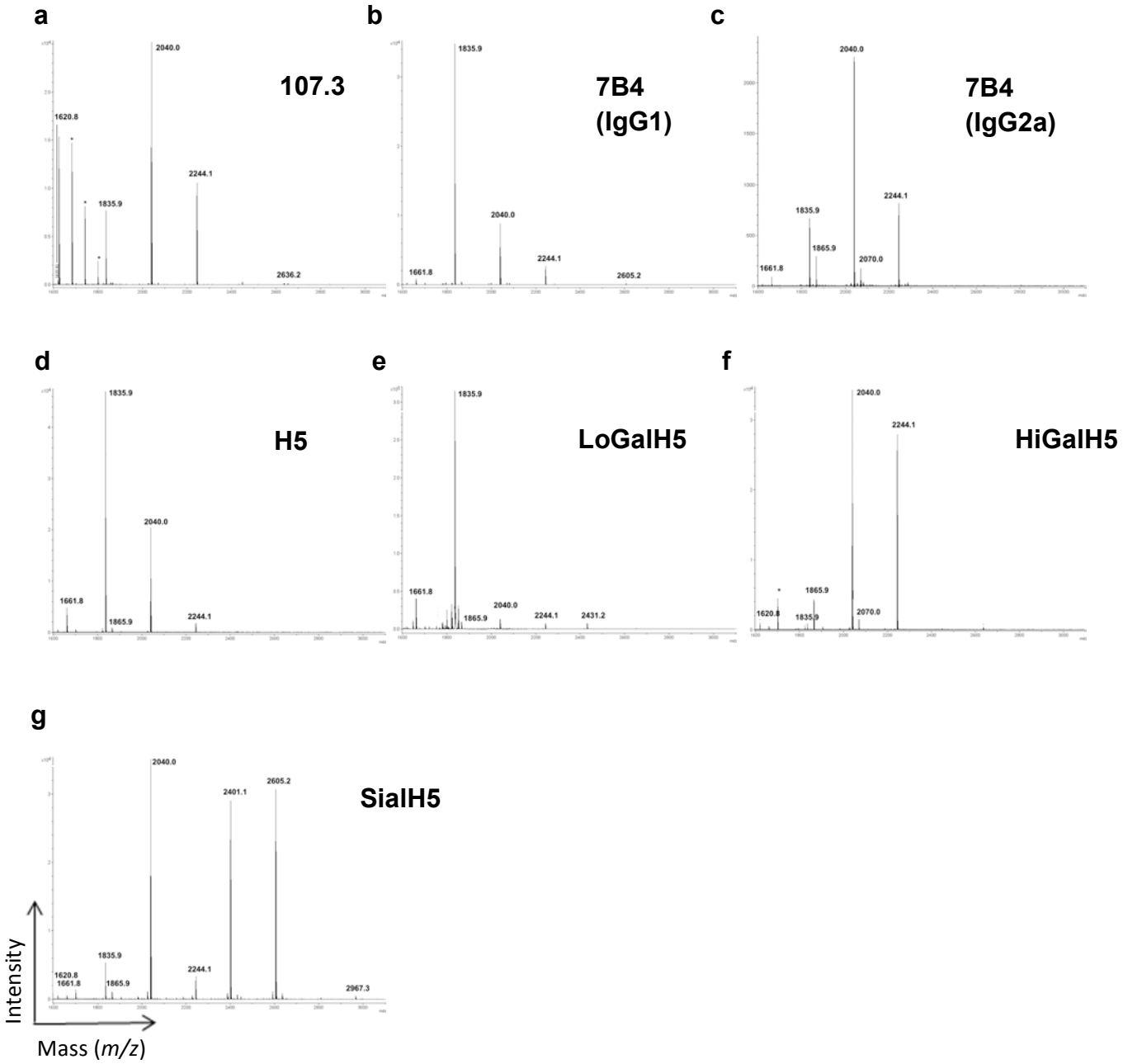

Supplementary Figure 12. MALDI-TOF spectra of N-glycans released from Asn297 of different TNP-specific antibodies after PNGase F digestion. N-glycan composition of (**a**) Ab 107.3 (IgG1; G1 and G2 = 81%), (**b**) Ab 7B4 (IgG1; G1 and G2 = 25.1%), (**c**) Ab 7B4 (IgG2a; G1 and G2 = 84.5%), (**d**) Ab H5 (IgG1; G1 and G2 = 30.3%), (**e**) *in vitro* degalactosylated Ab H5 (LoGalH5; IgG1; G1 and G2 = 8.8%), (**f**) *in vitro* galactosylated Ab H5 (HiGalH5, IgG1; G1 and G2 = 98.1 %); and (**g**) *in vitro* sialylated Ab H5 (SialH5; IgG1; G1 and G2 = 93.6%). Numbers indicate the molecular mass of released glycans, the 2D structures of which are depicted in Supplementary Fig. 11. *: contamination

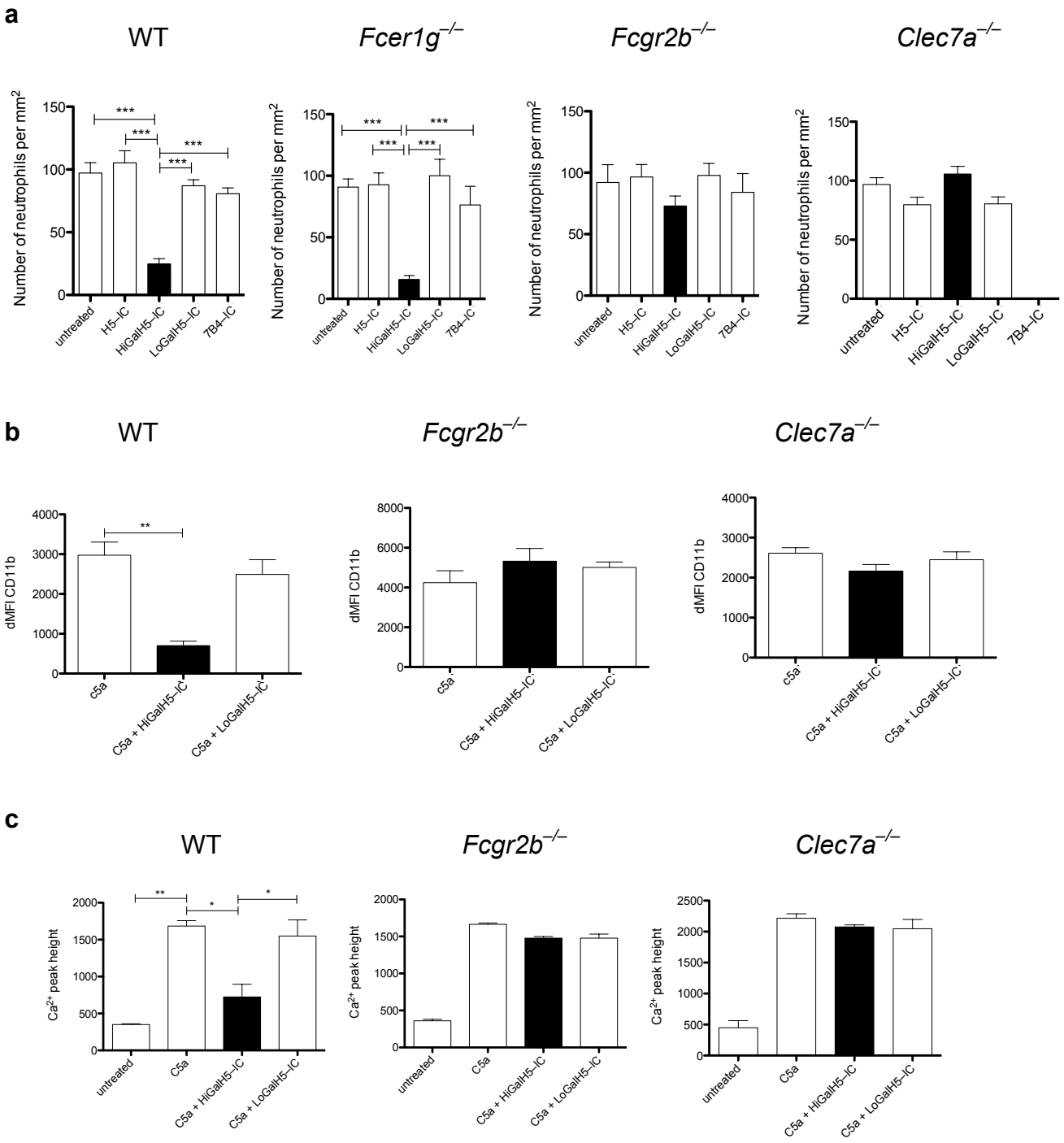

Supplementary Figure 13. Impact of HiGalH5–IC on C5a-mediated chemotaxis, upregulation of CD11b and increase in $[Ca^{2+}]_i$. (**a**), BM cells from the indicated mouse strains were treated with either H5–, HiGalH5–, LoGalH5– or low galactosylated 7B4 IgG1–IC. HiGalH5– but not LoGalH5–IC or 7B4–IC inhibit C5a-mediated chemotaxis of neutrophils from WT and *Fcerg1*$^{-/-}$ mice. HiGalH5–IC exert no inhibitory effect on neutrophils from *Fcgr2b*$^{-/-}$ or *Clec7a*$^{-/-}$ mice. (**b**) HiGalH5–IC suppress C5a-mediated upregulation of CD11b expression on WT but not on neutrophils from *Fcgr2b*$^{-/-}$ or *Clec7a*$^{-/-}$ mice. LoGalH5–IC exert no inhibitory effect. dMFI CD11b: increase in MFI mediated by the indicated treatment as compared with untreated control. (**c**) C5a-mediated increase in $[Ca^{2+}]_i$ is blocked by HiGalH5–IC in BM cells from WT mice but not from *Fcgr2b*$^{-/-}$ or *Clec7a*$^{-/-}$ mice. (*n*=3/group). Data are means $\pm$ s.e.m. **P*<0.05, ** *P*<0.01, *** *P*<0.001.

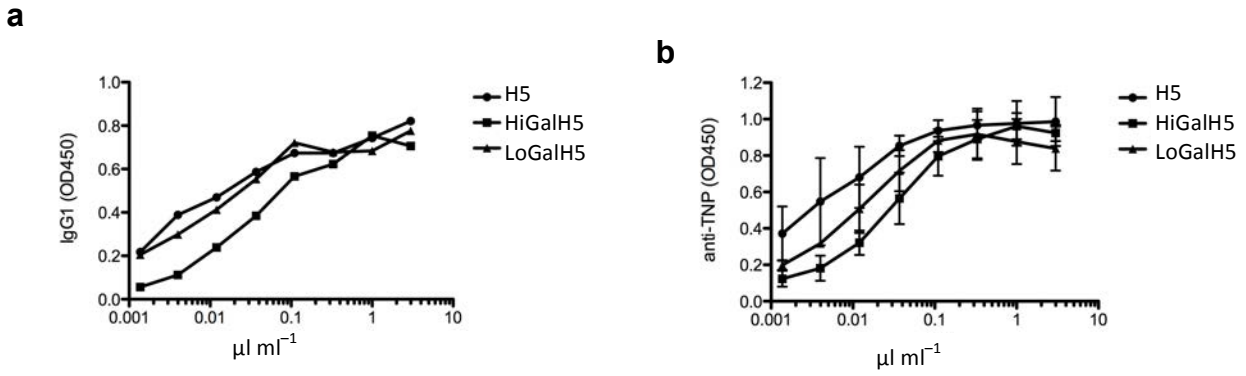

Supplementary Figure 14. In vitro galactosylation or degalactosylation of TNP-specific IgG1 H5 does not influence antigen binding. (**a**) Mouse IgG1 ELISA of naïve H5 Ab, *in vitro* galactosylated (HiGalH5) and *in vitro* degalactosylated (LoGalH5) TNP-specific IgG1 Abs. ELISA plates were coated with polyclonal mouse IgG1-specific Ab and developed with polyclonal mouse-specific IgG1 coupled to horseradish peroxidase. (**b**)**,** TNP reactivity of H5, HiGalH5 and LoGalH5 TNP-specific IgG1 Abs (*n*=3/group).

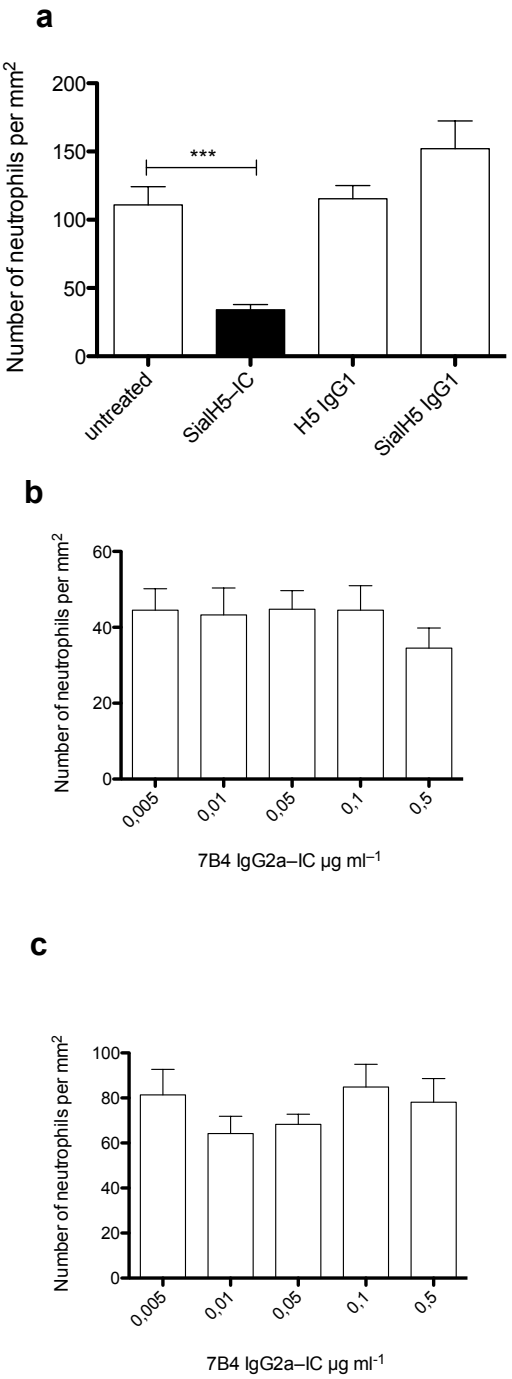

Supplementary Figure 15. Impact of sialylated IgG1 H5 (SialH5)–IC, monomeric H5 IgG1– and 7B4 IgG2a–IC on C5a-mediated chemotaxis. (**a**) BM cells from WT mice were incubated with SialH5–IC, H5 IgG1 or SialH5 IgG1 Abs for 30 min. The result shows that (i) sialylation does not affect the inhibitory effect of HiGalH5–IC; and (ii) IC formation of IgG1 Abs is essential for the inhibitory effect. Of note, the sialyltransferase almost completely sialylated the bi-galactosylated glycans (26% out 29%) but only a fraction of the mono-galactosylated glycans (26% of 64%). At this point, we cannot exclude that a higher sialylation of mono-galactosyalated glycans would alter the inhibitory effect of highly galactosylated H5–IC. Highly galactosylated TNP-specific IgG2a 7B4–IC do not block C5a-mediated migration of BM neutrophils from (**b**) WT or (**c**) *Fcer1g*$^{-/-}$ mice.

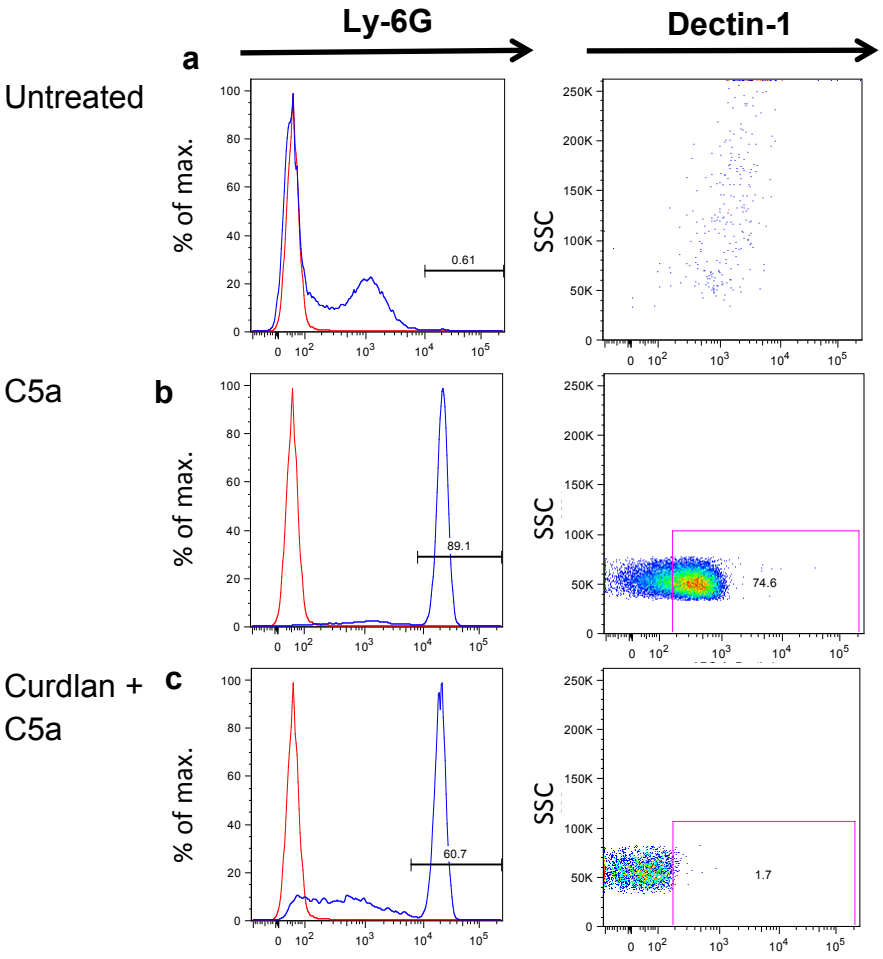

Supplementary Figure 16. Curdlan pretreatment abolishes Dectin-1 expression on neutrophils that migrated into the peritoneal cavity in response to C5a. (**a**) Percentage of Ly-6G^{hi} cells (left panel) in naive WT BALB/c mice and their expression of Dectin-1 (right panel). (**b**) as in **a**, except that mice were treated with C5a (200 nM, i.p.) for 6h. Here, 74.6% of Ly-6G^{hi} neutrophils that migrated into the peritoneum express Dectin-1. (**c**) as in **b**, except that mice were pretreated with curdlan (100 µg, i.v.) 30 min prior to C5a injection. Please note that only 1.7% of Ly-6G^{hi} neutrophils express Dectin-1. Results are representative of at least three independent experiments.

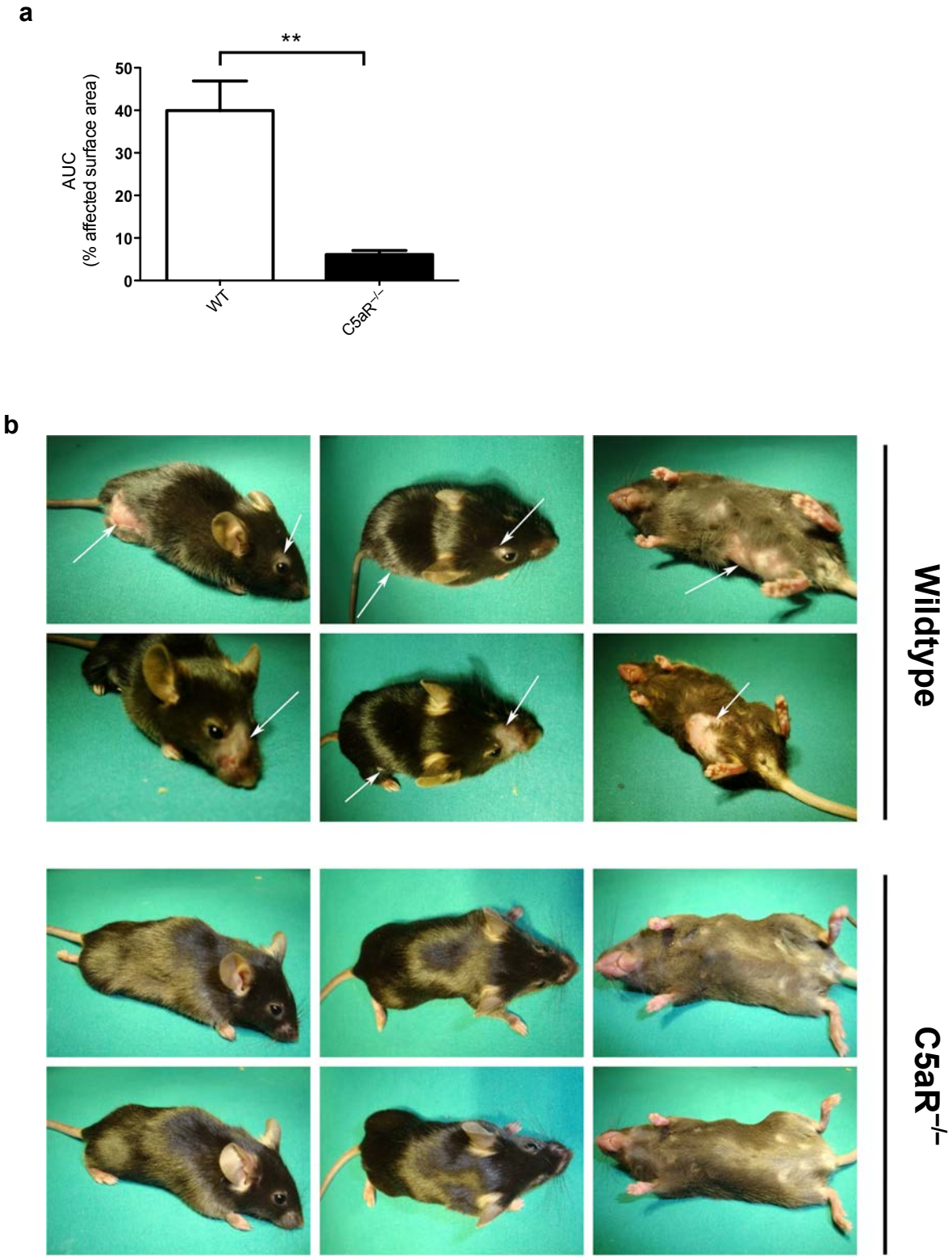

Supplementary Figure 17. C5aR deficiency protects from disease development in experimental epidermolysis bullosa acquisita (EBA). (**a**) Determination of the clinical severity during the course of experimental EBA from d4-12 by assessment of the area under the curve (AUC). (**b**) Clinical phenotypes of two representative mice from the WT and the C5aR$^{-/-}$ group are depicted on d12 after anti-collagen type VII IgG treatment. C57BL/6 mice developed widespread blistering skin disease (cutaneous lesions indicated by white arrows). In contrast, C5aR$^{-/-}$ mice were almost completely protected from EBA development. Data are means $\pm$ s.e.m. (n = 5-9/group).

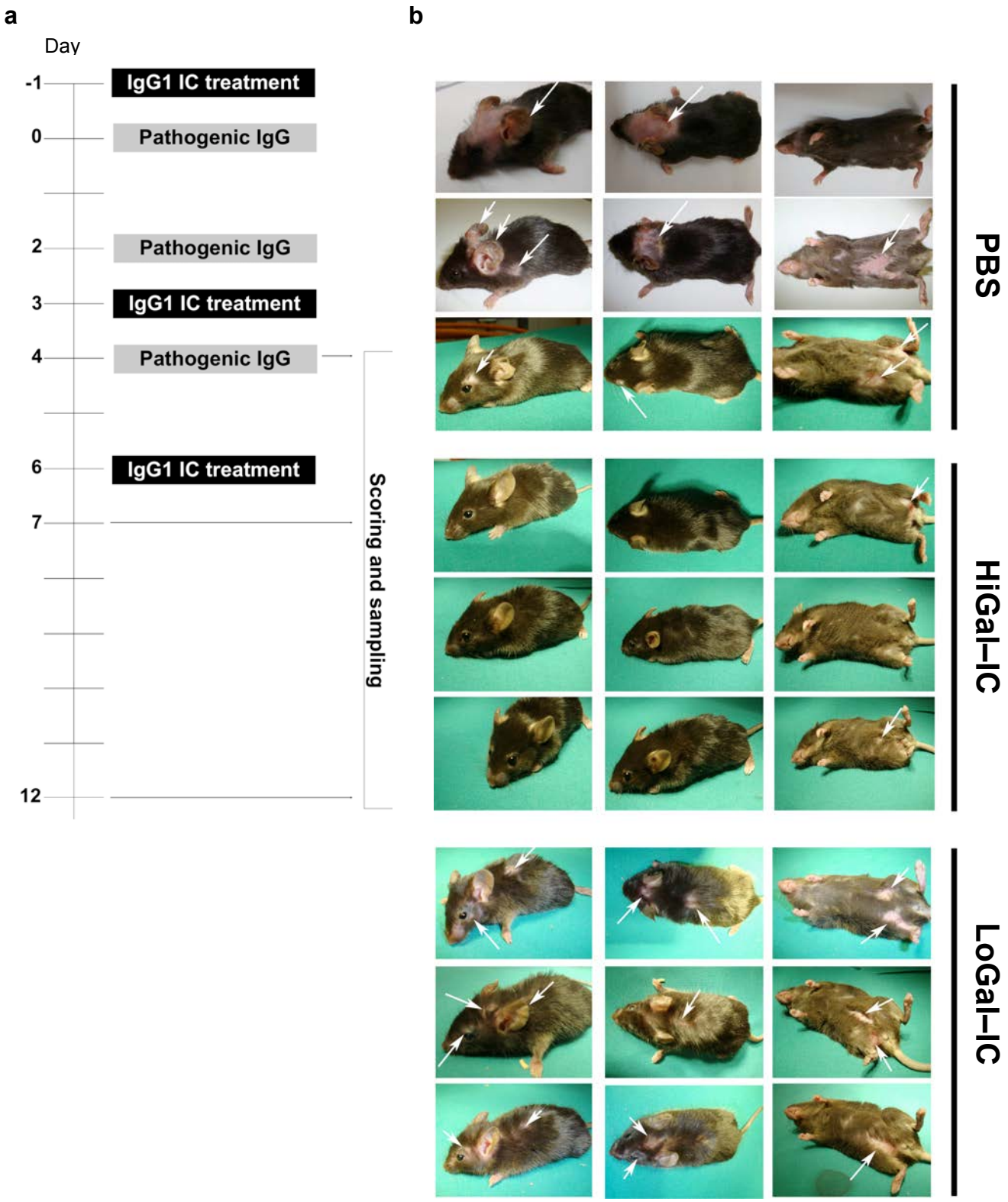

Supplementary Figure 18. HiGalH5–IC reduce the clinical severity of experimental EBA induced by transfer of rabbit IgG directed against murine collagen type VII. (**a**) Protocol underlying the model of experimental EBA and IgG1–IC treatment scheme. (**b**) Clinical phenotype of three representative mice from each treatment group (PBS, HiGalH5- and LoGalH5–IC) on d12 after anti-collagen type VII IgG injection is depicted. Mice treated with PBS or LoGalH5–IC developed widespread cutaneous lesions typical for experimental EBA. They are characterized by alopecia, blisters, erosions, epidermal detachment and crust formations. We observed lesions preferentially in the facial area, at the ears, the neck and the ventral site of the mice (as indicated by white arrows). In HiGalH5–IC-treated mice, such lesions were reduced in quantity and size.

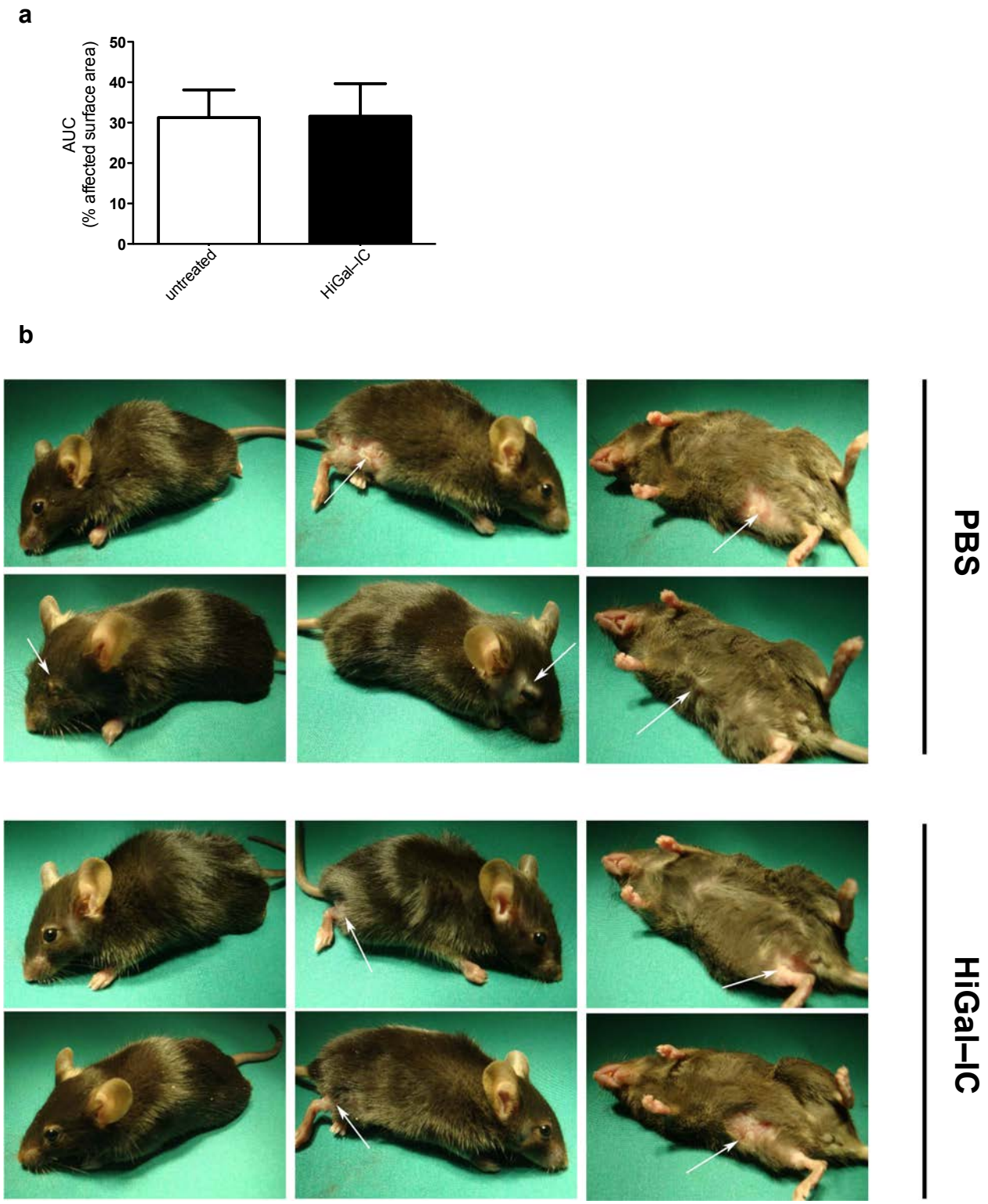

Supplementary Figure 19. HiGal–IC do not reduce the clinical severity of experimental EBA in *Clec7a*$^{-/-}$ mice. (**a**) Determination of the clinical severity during the course of experimental EBA from d4-12 by assessment of the area under the curve (AUC) in untreated and HiGal–IC-treated *Clec7a*$^{-/-}$ mice. (**b**) Clinical phenotypes of two representative *Clec7a*$^{-/-}$ mice from the untreated and the HiGal–IC-treated groups are depicted on d12 after anti-collagen type VII IgG treatment. Mice from both treatment groups developed comparable cutaneous lesions (in quantity and size) typical for experimental EBA as indicated by white arrows. Data are means $\pm$ s.e.m. (*n* = 6-7/group).

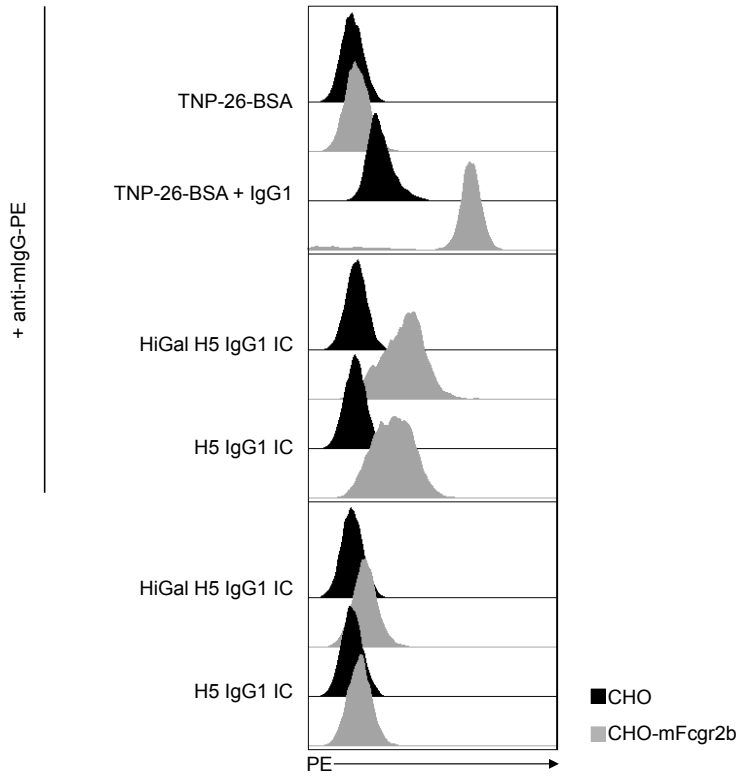

Supplementary Figure 20. H5–IC bind to FcγRIIB independent of the degree of glycan galactosylation. HiGalH5– and H5–IC were incubated with CHO cells (black) or CHO cells transfected with mouse FcγRIIB (CHO–*mFcgr2b*, grey) and stained for FcγRIIB binding using PE-labeled murine IgG-specific Ab. As positive control, CHO or CHO–*mFcgr2b* cells were stained with ICs composed of TNP-26 BSA and a TNP-specific IgG1–Ab. As negative control, CHO or CHO–*mFcgr2b* cells were incubated with HiGalH5– or H5–IC only (lower four histograms). Results are representative of two independent experiments.

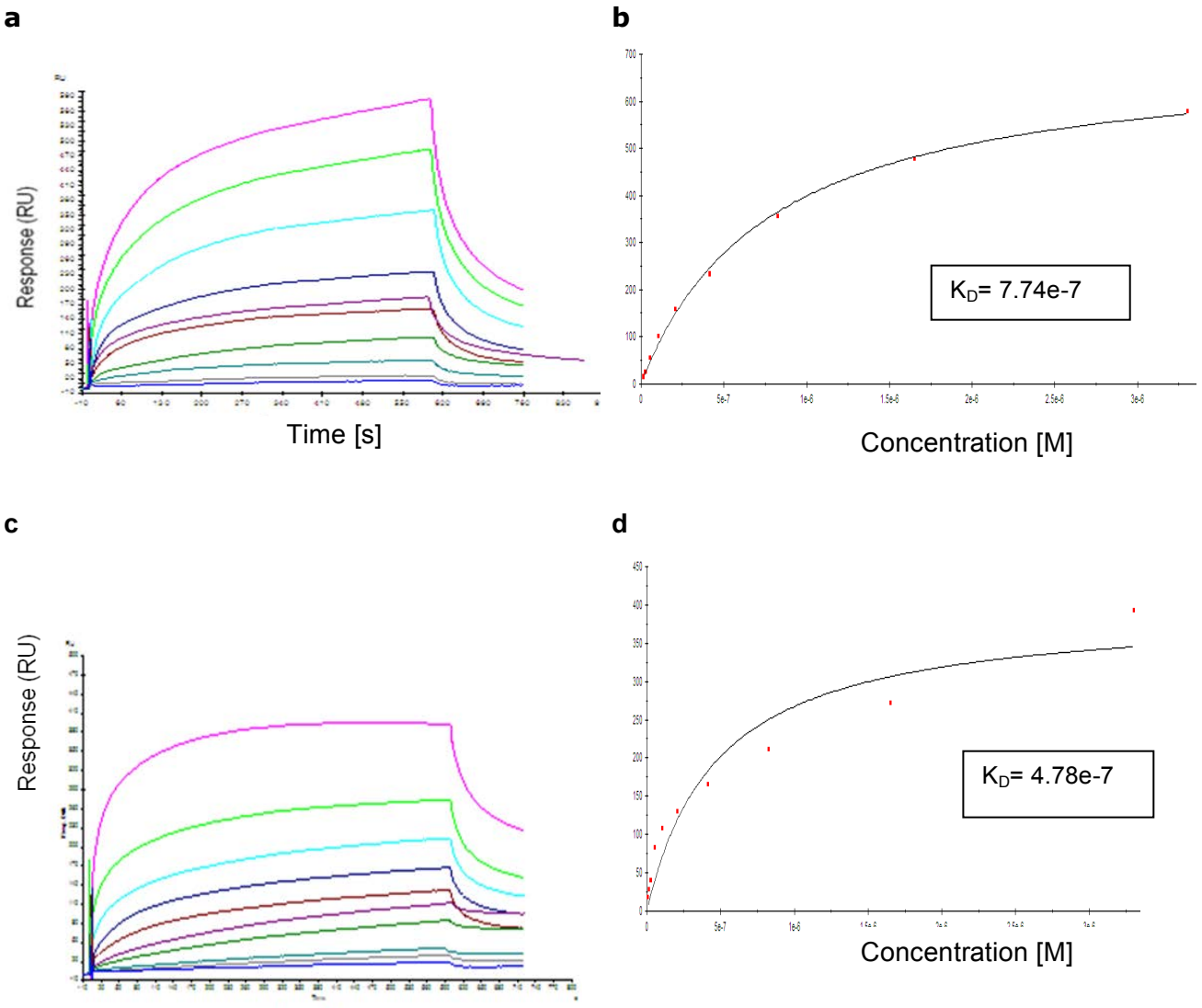

Supplementary Figure 21. Surface plasmon resonance interaction analysis of HiGalH5– and LoGalH5–IC with FcγRIIB. The binding of HiGalH5-IC (**a** and **b**) and LoGalH5-IC (**c** and **d**) to recombinant mouse FcγRIIB-Fc was analyzed using surface plasmon resonance. Ten serial dilutions of IC (1:2) were prepared starting at $1x10^{-8}$M (pink curves in **a** and **c**) and binding curves were determined. The equilibrium response (RU increase) was plotted against the concentrations of HiGalH5– (**b**) or LoGalH5–IC (**d**) to create a saturation curve of analyte binding and to calculate the dissociation constant (K_D).

a

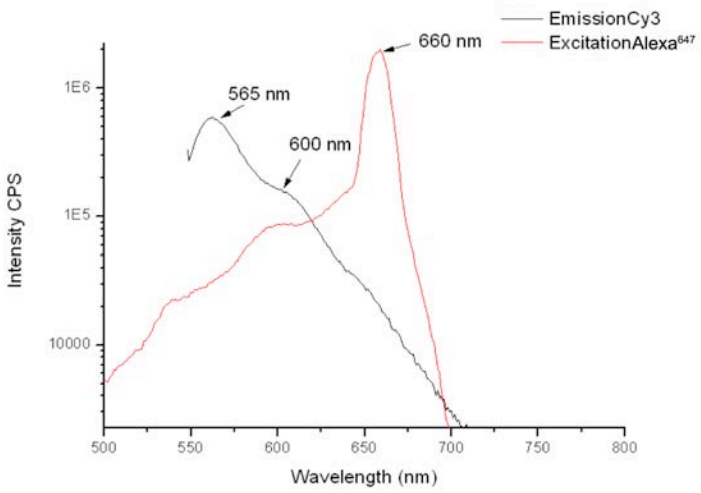

b

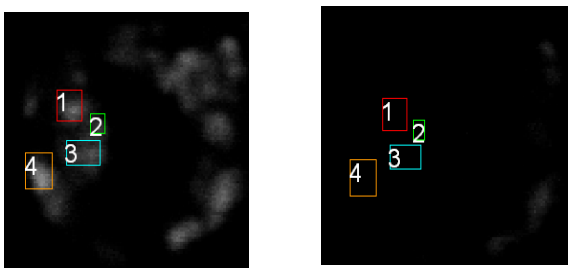

Supplementary Figure 22. Assessment of the requirements for FRET using Cy3 labeled HiGalH5–IC and Alexa647-labeled Dectin-1-specific Ab. (**a**) Spectral overlap of absorption spectrum for Alexa647-labeled Dectin-1 Ab acceptor and emission spectrum for Cy3-labeled HiGalH5–IC donor. (**b**) Single cell image of a neutrophil before (left) and after (right) acceptor bleach with four highlighted regions of interest.

a

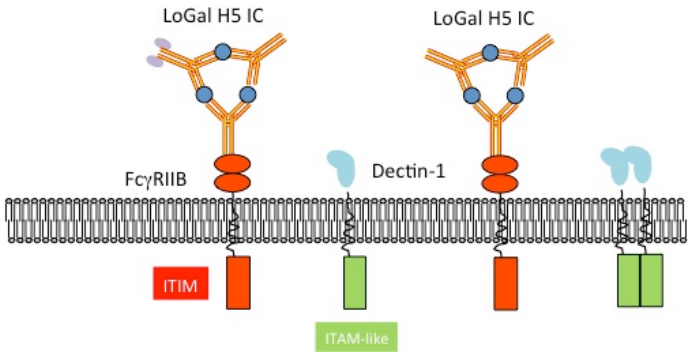

b

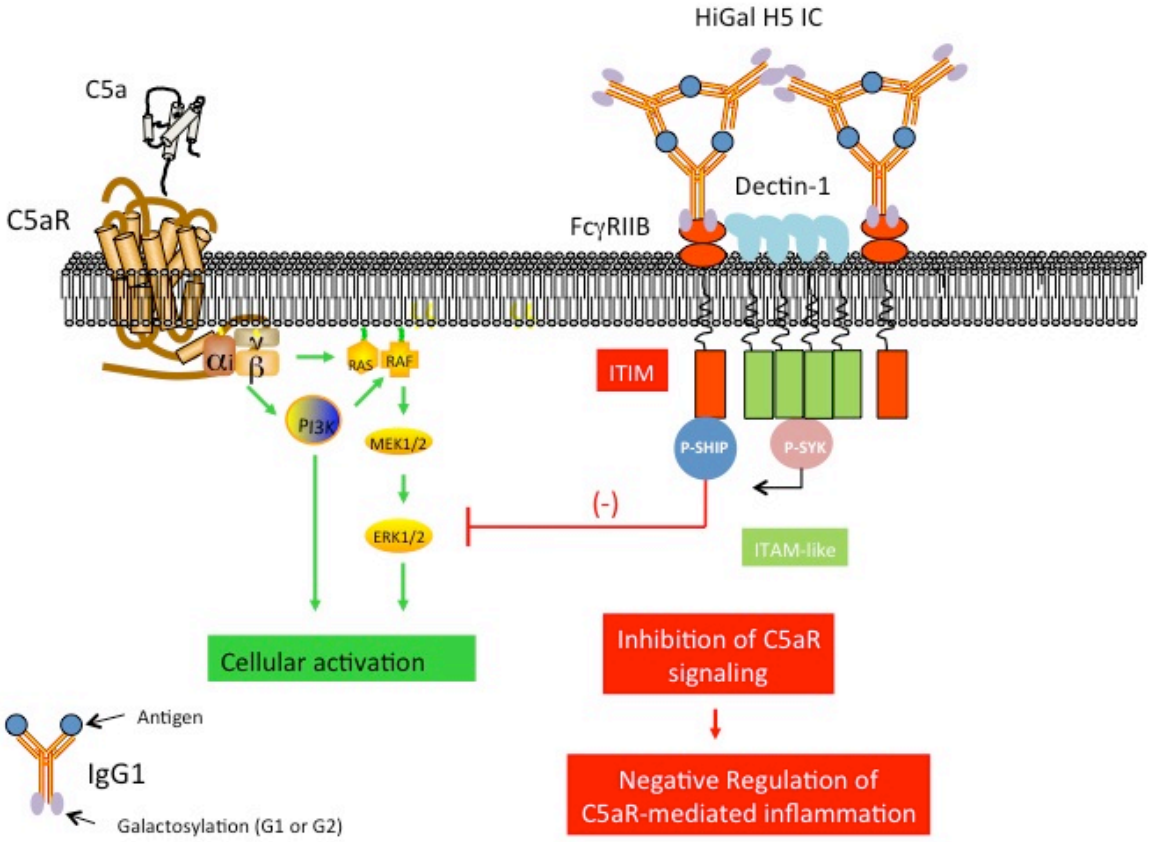

Supplementary Figure 23. Two step model by which highly galactosylated IgG1-IC associate FcγRIIB with Dectin-1 and inhibit C5aR signaling. a, IgG1-IC bind to FcγRIIB independent of their N-glycan galactosylation. Low or agalactosylated IgG1–IC such as LoGalH5–IC do not drive association of FcγRIIB with Dectin-1. **b**, Highly galactosylated IgG1 IC such as HiGalH5–IC link FcγRIIB to Dectin-1 resulting in tyrosine phosphorylation of the ITAM-like motif downstream of Dectin-1 and transient phosphorylation of Syk. Further, HiGalH5–IC drive the association of SHIP with the ITIM within FcγRIIB and its phosphorylation. This pathway inhibits C5a-mediated ERK1/2 phosphorylation and several cellular effector functions of C5aR.

		Antibody clone						
Mass	**107.3**	**7B4 (IgG1)**	**7B4 (IgG2a)**	**H5**	**LoGal H5**	**HiGal H5**	**SialH5**	**Galactose/ Sialic acid**
1620.8	1.03	0.47	0.20	0.61	-	1.24	0.53	**A1G1**
1661.8	0.18	1.13	1.65	5.68	10.03	0.67	0.55	**G0**
1835.9	16.97	73.78	13.64	64.00	81.17	1.20	5.34	**G0**
1865.9	0.49	0.82	5.81	1.04	2.44	5.78	1.13	**G1**
2040.0	58.81	18.64	54.47	26.62	3.30	50.61	36.85	**G1**
2070.0	0.37	0.54	4.24	-	-	1.96	0.11	**G2**
2244.1	22.15	4.62	19.99	2.05	1.67	38.54	2.81	**G2**
2401.1	-	-	-	-	-	-	26.11	**G1S1**
2431.2	-	-	-	-	1.39	-	-	**G1S1**
2605.2	-	-	-	-	-	-	26.57	**G2S1**
2636.2	-	-	-	-	-	-	-	**G2S1**
2967.3	-	-	-	-	-	-	-	**G2S2**
3026.5	-	-	-	-	-	-	-	**G2S2**
Total	100	100	100	100	100	100	100	

Supplementary Table. Composition of the glycans released from N297 of the indicated TNP-specific antibody clones after PNGase F digestion. The numbers on the left indicate the molecular mass of the different N-glycans as determined by MALDI-TOF. On the right, the number of terminal Gal residues (0=G0; 1=G1; and 2=G2) and sialic acid residues (Neu5Ac of human in blue and Neu5Gc mouse in red; 1=S1 and 2=S2) is depicted. For N-glycan 2D-structures, please refer to Supplementary Fig. 11. The numbers below each Ab clone depict the percentages of each individual glycan structure. The molecular mass of 3026.5 for the mouse G2S2 structure is the calculated mass.

Supplementary Methods

Surface Plasmon Resonance Analysis (SPR). To determine the interactions between FcγRIIB with HiGal– and LoGalH5–IC, SPR was performed using a Biacore 3000 (GE Healthcare) system at 25°C. FcγRIIB was coupled to the CM5 sensor chip (GE Healthcare) via amine coupling. For activation of the carboxylated dextran matrix of the CM5 chip, 0.05 M N-hydroxysuccinimide and 0.2 M N-ethyl-N'-(dimethylamino-propyl) carbodiimide in equal volumes were added to the sensor chip. For immobilization, FcγRIIB was diluted to 34µg ml^{-1}. Injection of 5µl receptor resulted in signal increase of 6000 resonance units (RU). Unbound reactive groups were saturated with 1 M ethanolamine hydrochloride-NaOH for 7min. A second flow chamber was subjected to the immobilization protocol but without any addition of protein and served as a reference cell. Serial dilutions of HiGalH5– or LoGalH5–IC in PBS were added (starting at 10 nM). For detection of association, the samples were passed over the sensor chip at a constant flow rate of 15µl min^{-1} for 10min. BIAevaluation software 3.2 RC1 was used for analysis of the data. First, the binding curves for the different dilutions were overlaid and the equilibrium response was determined. Then, the equilibrium response of each experiment was used to create saturation curves of analyte binding and to calculate the dissociation constant (KD) assuming a 1:1 steady state affinity model.

Supplementary Video 1. Expression of FcγRIIB but absence of Syk phosphorylation in untreated BM neutrophils. This movie shows the expression pattern of FcγRIIB (green, anti-FcγRIIB-FITC Ab) and of phosphorylated Syk (p-Syk, magenta, anti-p-Syk-Alexa568 Ab) in a BM-derived neutrophil 3min after incubation with PBS as determined by confocal microscopy in an animated three-dimensional projection. Cell stains positive for FcγRIIB. No phosphorylation of Syk is visible in the absence of 107.3–IC treatment. Similar results were obtained for p-SHIP.

Supplementary Video 2. Expression of Dectin-1 but absence of Syk phosphorylation in untreated BM neutrophils. This movie shows the expression pattern of Dectin-1 (magenta, anti-Dectin-1-APC Ab) and phosphorylated Syk (p-Syk, green, anti-p-Syk-Alexa568 Ab) in a BM-derived neutrophil 3min after incubation with PBS as determined by confocal microscopy in an animated three-dimensional projection. No phosphorylation of Syk occurs in the absence of 107.3–IC treatment. Similar results were obtained for p-SHIP.

Supplementary Video 3. Phosphorylation of Syk and co-localization of p-Syk with FcγRIIB in response to 107.3–IC treatment. This movie shows the co-localization pattern of FcγRIIB (green, anti-FcγRIIB-FITC Ab) and of phosphorylated Syk (p-Syk, magenta, anti-p-Syk-Alexa568 Ab) in a BM-derived neutrophil 3min following 107.3–IC treatment as determined by confocal microscopy in an animated three-dimensional projection. 107.3–IC treatment drives phosphorylation of Syk; p-Syk co-localizes with FcγRIIB as indicated by the white spots. Similar results were obtained for p-SHIP.

Supplementary Video 4. **Phosphorylation of Syk and co-localization of p-Syk with Dectin-1 in response to 107.3–IC treatment.** This movie shows the co-localization pattern of Dectin-1 (magenta, anti-Dectin-1-APC Ab) and phosphorylated Syk (p-Syk, green, anti-p-Syk-Alexa568 Ab) in a BM-derived neutrophil 3min following 107.3–IC treatment as determined by confocal microscopy in an animated three-dimensional projection. 107.3–IC treatment drives phosphorylation of Syk; p-Syk co-localizes with Dectin-1 as indicated by the white spots. Similar results were obtained for p-SHIP.

Supplementary Video 5. 107.3–IC treatment promotes association of FcγRIIB and Dectin-1. This movie shows the co-localization pattern of FcγRIIB (green, anti-FcγRIIB-FITC Ab) and of Dectin-1 (magenta, anti-Dectin-1APC Ab) in a BM-derived neutrophil 3min after incubation with 107.3–IC as determined by confocal microscopy in an animated three-dimensional projection. Co-localization of FcγRIIB and Dectin-1 is indicated by the white spots.